

LECTURE NOTES ON QUANTUM TEICHMÜLLER THEORY.

LEONID CHEKHOV.

Notes collected by M. Mazzocco

ABSTRACT. These notes are based on a lecture course by L. Chekhov held at the University of Manchester in May 2006 and February-March 2007. They are divulgative in character, and instead of containing rigorous mathematical proofs, they illustrate statements giving an intuitive insight. We intentionally remove most bibliographic references from the body of the text devoting a special section to the history of the subject at the end.

CONTENTS

1. Combinatorial description of Teichmüller spaces	1
2. Coordinates in the Teichmüller space	8
3. Modular group action	13
4. Poisson brackets	17
4.1. Relations between geodesic functions	18
5. Quantization	20
6. Bibliographic references	23
Appendix A. The hyperbolic metric	24
Appendix B. Poisson brackets between geodesic functions	25
References	27

1. COMBINATORIAL DESCRIPTION OF TEICHMÜLLER SPACES

In this lecture we concentrate on the Teichmüller space \mathcal{T}_g^s of Riemann surfaces $F_{g,s}$ of genus g with s holes.

Example 1.1. The simplest case is the torus with one hole, $F_{1,1}$ (see figure 1).

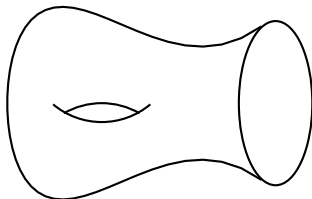


FIGURE 1. A torus with one hole

The holes can be considered in different parameterizations. For this lecture course we concentrate on the Poincaré uniformization. There is another uniformization which is due to Strebel, but in the Poincaré one there is a good description of the Poisson structure and of the quantization.

What is the Poincaré uniformization? On each $F_{g,s}$ we may define several metrics. We consider two metrics to be equivalent if they are mapped one to another by a diffeomorphism. Within each equivalence class, we chose the representative to be a metric with local constant curvature -1 . Observe that for $g > 1$ there always exists such representative element (i.e. we may pick $s = 0$). For $g = 1$ we need at least one hole, otherwise it is impossible as the universal cover of the torus is flat. For $g = 0$, we need at least $s = 3$.

This is called *Poincaré uniformization*: our Riemann surface $F_{r,s}$ is mapped to a surface with local constant curvature -1 , namely

$$F_{g,s} = \mathbb{H}/\Delta_{g,s},$$

where \mathbb{H} denotes the upper half plane and $\Delta_{g,s}$ is a *Fuchsian group*, i.e. a finitely generated discrete subgroup of the isometry group $\mathbb{P}SL(2, \mathbb{R})$ of \mathbb{H} :

$$\Delta_{g,s} = \langle \gamma_1, \dots, \gamma_{2g+s} \rangle,$$

where $\gamma_1, \dots, \gamma_{2g+s}$ are *hyperbolic elements*, i.e. they have two distinct fixed points on the *absolute*, i.e. $\mathbb{R} \cup \{\infty\}$.

Recall that on \mathbb{H} we have the metric $ds^2 = \frac{dx^2 + dy^2}{y^2}$ and the geodesics are either semi-circles with centre on the x -axis or half-lines parallel to the y -axis (see figure 2). To familiarize the reader with the hyperbolic metric, we have discussed some examples in Appendix A.

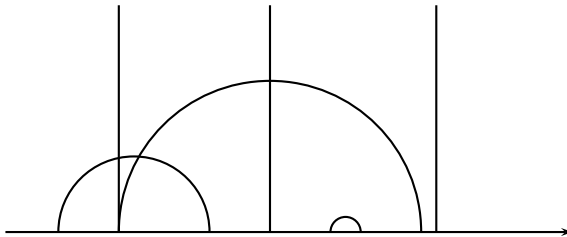


FIGURE 2. Some geodesics in the upper half plane

Observe that given a geodesic γ and a point P in \mathbb{H} not belonging to it, there are infinitely many geodesics through P which do not cross γ (therefore Euclid's postulate does not hold true in hyperbolic geometry). The x -axis is infinitely distant from the points in \mathbb{H} , this is why we say that it belongs to the *absolute*.

Note that actually, no "points" lie on the absolute; instead we consider classes of geodesics terminating at such a point in a sense that all of them become asymptotically close at large proper distances: the collection of such "points" is the open real line together with the infinity point (defined by upper ends of vertical geodesic lines: all these lines in Fig. 2 are asymptotically close). The equivalent and often used picture is the Poincaré disc: the absolute is the boundary of the disk and the geodesics are arcs.

Let $A \in \mathbb{P}SL(2, \mathbb{R})$ with $A = \begin{pmatrix} a & b \\ c & d \end{pmatrix}$. This acts on \mathbb{H} by the Möbius transformation

$$\gamma_A : z \mapsto \frac{az + b}{cz + d}.$$

This action is *transitive*, and the Möbius transformation has two fixed points (possibly at infinity), given by

$$z_{\pm} = \frac{1}{2c} \left(a - d \pm \sqrt{T^2 - 4} \right),$$

where $T = \text{trace}(A)$. If one fixed point is at ∞ (i.e. if $c = 0$) then the other is at $b/(d - a) \in \mathbb{R}$. Notice that T is not well-defined on $\mathbb{P}SL(2, \mathbb{R})$ but T^2 is. Analogously, the ratio $\frac{a-d}{c}$ is well defined in $\mathbb{P}SL(2, \mathbb{R})$, so the fixed points are indeed uniquely determined by the element in $\mathbb{P}SL(2, \mathbb{R})$. Two non-identity elements in $\mathbb{P}SL(2, \mathbb{R})$ commute if and only if they have the same fixed points.

The element $A \in \mathbb{P}SL(2, \mathbb{R})$ is said to be *hyperbolic* if $T^2 > 4$, *elliptic* if $T^2 < 4$ and *parabolic* if $T^2 = 4$. Parabolic elements have a unique fixed point on the absolute, and are conjugate to $\begin{pmatrix} 1 & 1 \\ 0 & 1 \end{pmatrix}$.

We will almost exclusively be interested in hyperbolic elements. The fixed points of such elements are real (lie on the absolute). Since the Möbius transformation γ_A is a hyperbolic isometry, it follows that it preserves the unique geodesic between its two fixed points. We call such geodesic *invariant axis*.

The eigenvalues of the matrix A are given by

$$\lambda_{\pm} = \frac{1}{2} \left(T \pm \sqrt{T^2 - 4} \right).$$

The linearization of the Möbius transformation γ_A , at the fixed point z_{\pm} is the complex linear map with eigenvalue λ_{\pm}^2 .

Given any element $\gamma \in \mathbb{P}SL(2, \mathbb{R})$, $\gamma = \begin{pmatrix} a & b \\ c & d \end{pmatrix}$, $ad - bc = 1$, we can uniquely determine it by its eigenvalues and its eigenvectors. We are now going to characterize γ by two other objects: a closed geodesic and its length.

In fact, since the determinant of γ is one, the eigenvalues can be expressed as $\exp\left(\pm \frac{l_{\gamma}}{2}\right)$. In the basis of the eigenvectors, $\gamma(z) = \exp(l_{\gamma})z$, so γ is a dilation and because it must be an isometry, it maps the whole geodesic through z to a second geodesic (see figure 3).

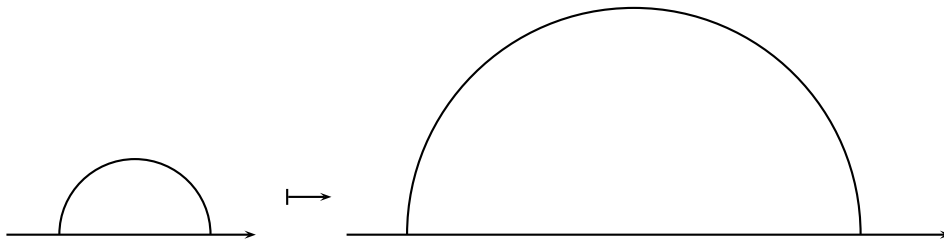


FIGURE 3.

Our diagonalized element γ has two distinct fixed points which are 0 and ∞ . Generally if γ is not diagonal, the position of the fixed points is uniquely determined by the eigenvectors. They always lie on the absolute.

Example 1.2. Consider $\gamma = \begin{pmatrix} 2 & 2 \\ \frac{1}{2} & 1 \end{pmatrix}$, it has eigenvalues $\lambda_{\pm} = \frac{1}{2}(3 \pm \sqrt{5})$ and eigenvectors $v_{\pm} = (1 \mp \sqrt{5}, 1)$. So the fixed points lie at $z = 1 \mp \sqrt{5}$. The other geodesics are mapped as in figure 4.

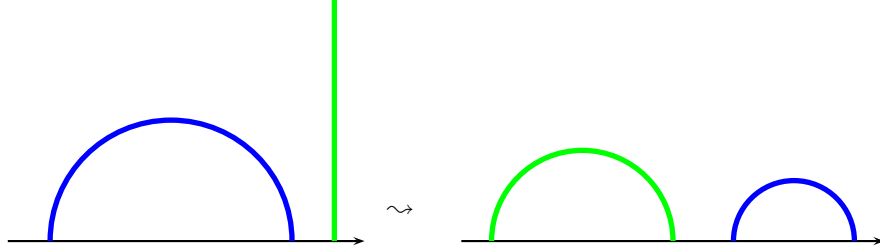


FIGURE 4.

If we identify points on \mathbb{H} by the action of γ , it means that we have to identify the initial geodesic and its image under γ , so that we obtain an infinite hyperboloid. Let us consider the only finite (i.e. not connecting points which lie on the absolute) geodesic contained between the initial geodesic and its γ -image. This is mapped to the only closed geodesic in our hyperboloid (figure 5).

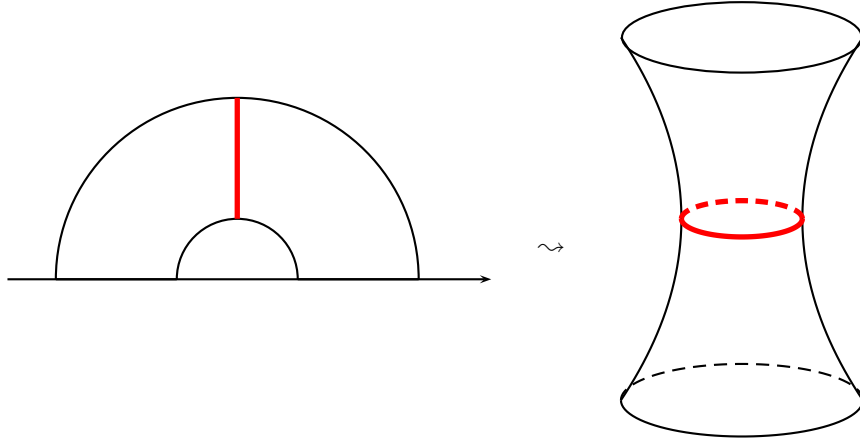


FIGURE 5.

The length of this closed geodesic is

$$\int_1^{l_\gamma} \frac{dy}{y} = l_\gamma,$$

where we have assumed for sake of simplicity that the initial geodesic had Euclidean radius one. So we see that for each hyperbolic element γ there exists a unique closed geodesic and its hyperbolic length is related to the trace of γ :

$$\text{Tr}(\gamma) = 2 \cosh l_\gamma.$$

As the trace is invariant under the action of $\mathbb{P}SL(2, \mathbb{R})$, the hyperbolic-length is a *hyperbolic-invariant*. Functions on \mathbb{H} which are invariant under the action of a Fuchsian group are called *automorphic functions*. Observe that the red closed geodesic lies on a geodesic of \mathbb{H} which relates two points: 0 and ∞ . These are exactly the stable points of γ .

Lemma 1.3. *Closed geodesics are in one-to-one correspondence with invariant axis of hyperbolic translations.*

Observe that actually we are interested in the Teichmüller space. Therefore the whole construction is invariant under the action of the automorphism group of \mathbb{H} , that is, $\mathbb{P}SL(2, \mathbb{R})$. The only relevant information about γ is that it has two distinct eigenvalues, and its trace. So we can state the following

Lemma 1.4. *The following objects are in one-to-one correspondence*

- (1) *Conjugacy classes of hyperbolic elements $\gamma \in \Delta_{g,s}$.*
- (2) *Closed geodesics on a Riemann surface; their lengths are related to the traces of γ .*

In virtue of the above lemma we shall often identify conjugacy classes of hyperbolic elements with their representative γ and we shall denote the associated closed geodesic in the same way, i.e. γ .

We now show that they are in one to one correspondence with the homotopy classes in $\pi_1(F_{g,s})$. In fact in each homotopy class we have only one shortest representative. Its length determines l_γ . Its topology determines the invariant points of γ .

To show this, we illustrate how to reconstruct the Riemann surface $F_{g,s}$ from the generators $\gamma_1, \dots, \gamma_n$ of the Fuchsian group $\Delta_{g,s}$. We do this in the simplest possible case, i.e. when there are only two hyperbolic generators, γ and $\tilde{\gamma}$. We assume that γ has fixed points 0 and ∞ as above and that $\tilde{\gamma}$ has fixed points on the x -axis. In both cases the geodesic connecting the fixed points is called *invariant axis*. The action of $\tilde{\gamma}$ on the geodesics is supposed to be like in example 1.2. To understand better let us draw the picture on the Poincaré disk. In this setting each arc is mapped in the opposite one and its *inside* (white domain) is mapped to the *outside* of the opposite one. In the figure 6 the green arc is mapped to the yellow one by $\tilde{\gamma}$. We draw also the same geodesics in the hyperbolic plane. The shaded area is the *fundamental domain*. In figure 7 we show the invariant axis.

We now glue as in figure 5, obtaining a hyperboloid. The yellow and green geodesic are drawn on the hyperboloid in figure 8. Since we are going to identify them, we draw them in the same colour (green). By gluing along the green geodesics we get our torus with one hole (see figure 8). Observe that in particular we can identify the red geodesic with an A -cycle and the blue one with a B -cycle. To remember this we shall denote

$$\gamma_A = \gamma, \quad \gamma_B = \tilde{\gamma}.$$

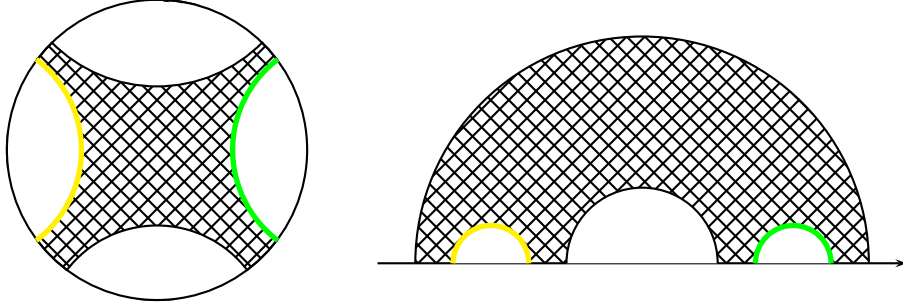
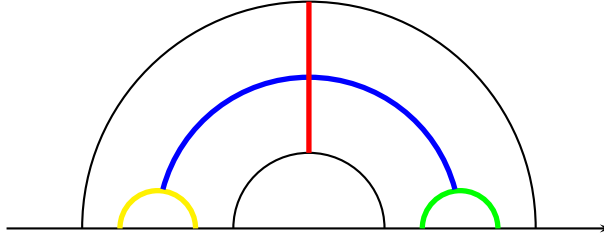


FIGURE 6.

FIGURE 7. The red invariant axis corresponds to γ , while the blue one to $\tilde{\gamma}$.

Once we have obtained our torus with one hole, it is clear that only the homotopy class of the closed geodesics corresponding to the invariant axes (i.e. the red and blue ones) are relevant.

Lemma 1.5. *The following objects are in one-to-one correspondence:*

- (1) *Conjugacy classes of hyperbolic elements $\gamma \in \Delta_{g,s}$.*
- (2) *Closed geodesics of given length.*
- (3) *Conjugacy classes in $\pi_1(F_{g,s})$.*

Finally we want to prove that all this is in one-to-one with the so called *fat-graph*. This is going to give us a combinatorial description of the Teichmüller space.

Usually graphs are determined by their incidence matrix specifying how many edges meet at each vertex. Suppose the faces carry an orientation. In order to be able to put an orientation on the edges which is compatible with the orientation of the faces, we make the graph fat, or ribbon. Moreover we shift each crossing so that at each vertex only 3 edges come together (see figure 9).

In this way, a curve coming from an edge at a vertex may turn either left or right (which makes all computations combinatorially simpler).

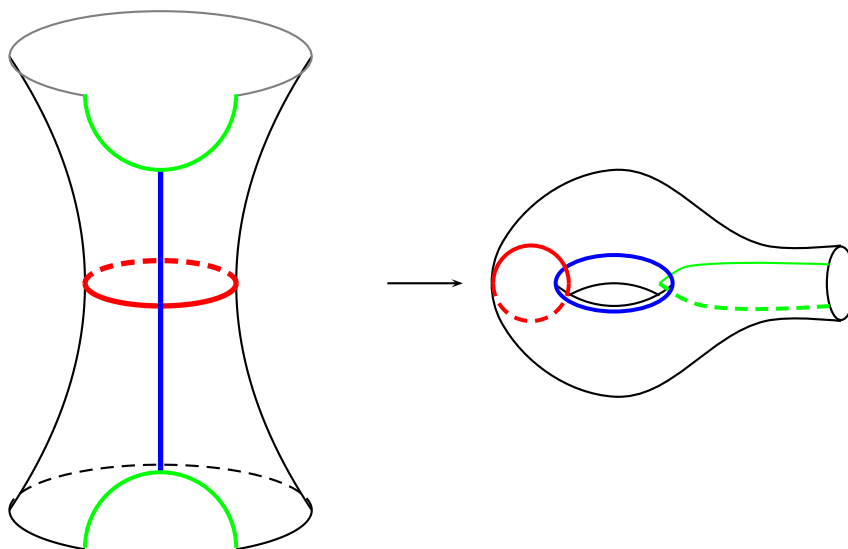


FIGURE 8. Glue along the green curve

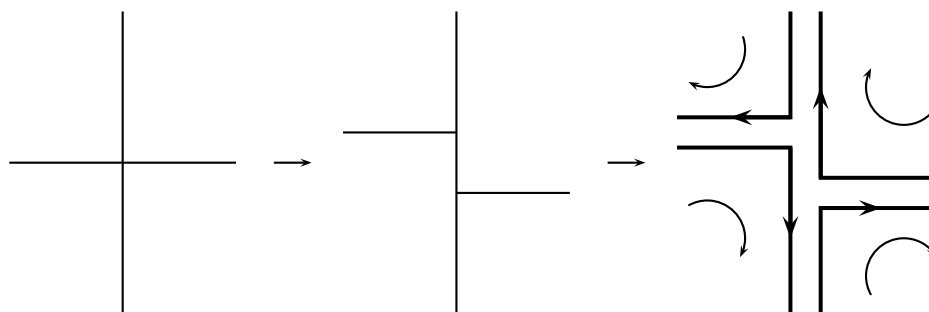


FIGURE 9. Resolving of a crossing into a fat graph

Now in our torus with one hole let us pick the graph defined by our A and B cycles and make it into a fat graph. Observe that the this fat graph has only one face and such face contains the hole (see figure 10).

So the rules for a fat graph are

- (1) The vertices are trivalent
- (2) Each face must contain only one hole.

For each such fat graph Γ there exists a unique Riemann surface for which Γ gives the minimal simplicial decomposition. Then we can add a fourth element in lemma 1.5:

Theorem 1.6. *The following objects are in one-to-one correspondence:*

- (1) *Conjugacy classes of hyperbolic elements $\gamma \in \Delta_{g,s}$.*
- (2) *Closed geodesics of given length.*

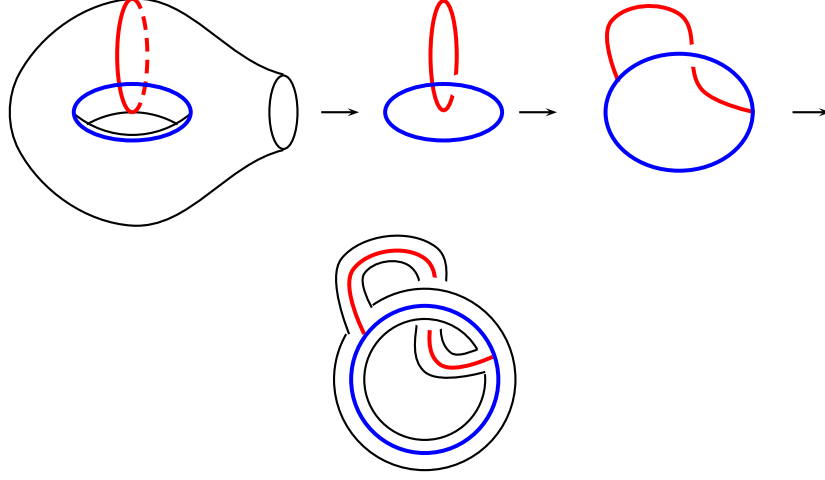


FIGURE 10. How to associate a fat-graph to a Riemann surface.

- (3) *Conjugacy classes in $\pi_1(F_{g,s})$.*
- (4) *Closed paths in a fat graph Γ .*

2. COORDINATES IN THE TEICHMÜLLER SPACE

We now want to find good coordinates in the Teichmüller space \mathcal{T}_g^s . Recall that each point in \mathcal{T}_g^s is specified by a Fuchsian group $\Delta_{g,s}$ generated by hyperbolic elements each of which is uniquely determined by its invariant axis in the fundamental domain. Given a hyperbolic element γ , we are going to express it as the product of matrices of type

$$L := \begin{pmatrix} 0 & 1 \\ -1 & -1 \end{pmatrix}, \quad R := \begin{pmatrix} 1 & 1 \\ -1 & 0 \end{pmatrix}, \quad X_z := \begin{pmatrix} 0 & -\exp(\frac{z}{2}) \\ \exp(-\frac{z}{2}) & 0 \end{pmatrix},$$

for some $z \in \mathbb{R}$. Projectively $R = L^2$ and $L = R^2$. We are looking for a decomposition of the form

$$\gamma = R^{k_n} X_{z_n} \dots R^{k_1} X_{z_1},$$

where k_i can be either 1 or 2. Observe that γ obtained in this way will necessarily be real and have the following sign structure

$$\text{sign}(\gamma) = \begin{pmatrix} + & - \\ - & + \end{pmatrix}$$

because each of the matrices RX_{z_i} and LX_{z_i} has this structure. This is not a restrictive condition, because we are taking $\gamma \in \mathbb{P}SL(2, \mathbb{R})$ with freedom of conjugation by $\mathbb{P}SL(2, \mathbb{R})$ as due to Theorem 1.6, only the conjugacy class of γ is relevant.

Example 2.1. Let us factorize an element of the Fuchsian group γ in the above way. Suppose γ maps

$$0 \rightarrow -1, \quad \exp(z_0) \rightarrow \infty, \quad \infty \rightarrow -1 - \exp(-z_1),$$

for some real numbers z_0, z_1 . It is a straightforward computation to show that

$$\gamma = RX_{z_1}LX_{z_0},$$

is the correct factorization.

We are now going to show a way to guess such factorization by constructing an *ideal triangulation* of the fundamental domain of the Riemann surface in which all the infinite hyperboloids attached to the holes have been cut off. More precisely, consider the closed curves homeomorphic to the holes, say the *bottleneck curves* on each hyperboloid. These are closed geodesics, therefore they correspond to an element of the Fuchsian group. In the case of one hole in the torus the image of the bottleneck curve in the fundamental domain is given in figure 11.

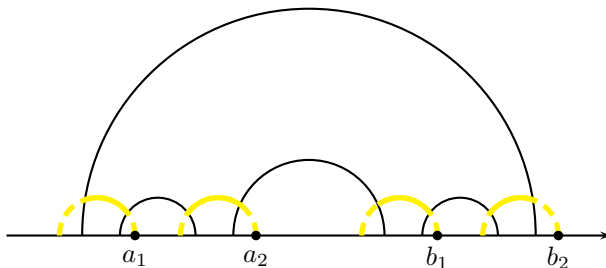


FIGURE 11. Image of the bottleneck curve in the fundamental domain.

Our new fundamental domain and its ideal triangulation will be determined by all the right (or all the left) points of the images of the bottleneck curve in \mathbb{H} laying on the absolute. In figure 11, these are a_1, a_2, b_1, b_2 and all their images under the action of the Fuchsian group $\Delta_{g,s}$. The fundamental domain and the ideal triangulation associated in this way to our torus with one hole are shown in figure 2.

To convince oneself that this new fundamental domain actually corresponds to the Riemann surface in which all the infinite hyperboloids attached to the holes have been cut off, consider the geodesic between a_2 and b_1 . This becomes an infinite (because a_2, b_1 lie on the absolute) geodesic on the Riemann surface that does not intersect the bottleneck curve (because the latter is not contained in the new fundamental domain) and therefore winds infinitely asymptotically approaching the bottleneck curve as in figure 13.

The new fundamental domain is then the finite collection of ideal triangles (for $F_{g,s}$ we have exactly $4g - 4 + 2s$ ideal triangles), which become, under the Fuchsian group action, the one-to-one covering of an *open* Riemann surface with all infinite hyperboloids removed (together with their bounding bottleneck curves, to be precise).

By the action of $\mathbb{P}SL(2, \mathbb{R})$, we can move a_1, a_2 and b_2 to $0, -1$ and ∞ respectively. So we can always label three of the points on the right side of each copy of the bottleneck curve by $-1, 0, \infty$. The fourth will be $\exp(z_0)$ for some real number z_0 . The element γ_B then maps $a_2 \rightarrow a_1, b_1 \rightarrow b_2, b_2 \rightarrow b_3$, that is $0 \rightarrow -1, \exp(z_0) \rightarrow \infty, \infty \rightarrow -1 - \exp(-z_1)$, as in example 2.1.

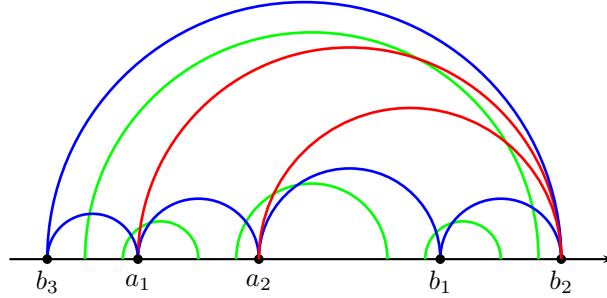


FIGURE 12. The new fundamental domain is the blue one. The ideal triangulation is obtained by the red geodesic. The old fundamental domain is shown in green.

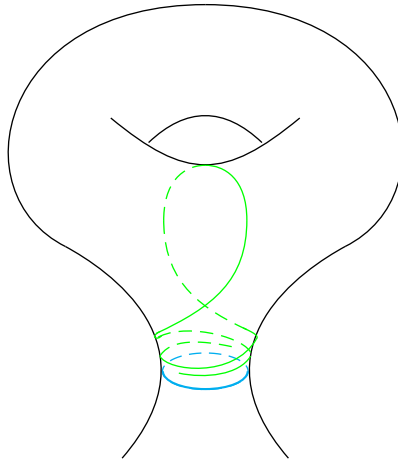


FIGURE 13. An example of a bounding geodesic asymptotically approaching the bottleneck curve.

Let us use the Poincaré disk model. We start from the initial triangle of vertices $0, e^{z_0}, \infty$. The transformation X_{z_0} maps ∞ to 0 , e^{z_0} to -1 and 0 to ∞ (see figure 14). That is, the initial triangle is mapped in the reference one. Now we want to reach the final triangle by the same type of transformation. To this aim, we need to rotate the reference triangle in clock wise direction. This is represented by the L matrix, or "left" matrix. In fact L maps ∞ to 0 , 0 to -1 and -1 to ∞ . Now apply X_{z_1} , i.e. 0 is mapped to ∞ , -1 to e^{z_1} and ∞ to 0 . Finally we need to apply a right rotation R to get back to the initial configuration of the reference triangle.

Opening up the same picture on \mathbb{H} we get again that the red triangle is mapped into the blue one through the reference one in the middle (see figure 15).

We can picture the same decomposition in the fat graph by assigning a label z_0, z_1, z_2 to each edge of the fat graph and choosing an orientation a priori. For example in figure 16 the decomposition of γ_B can be guessed by observing that

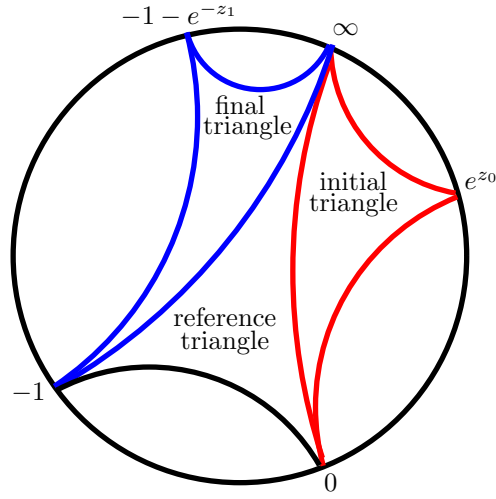


FIGURE 14.

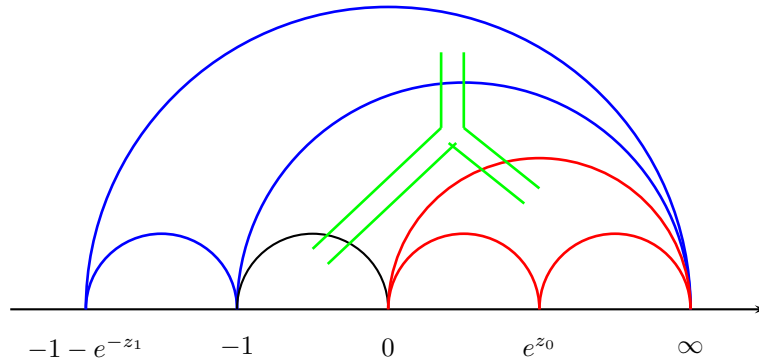


FIGURE 15.

starting from the z_0 edge of the fatgraph, the curve goes left into the z_1 edge and then right back into the z_0 edge.

In a similar manner we can obtain also $\gamma_A = LX_{z_2}RX_{z_0}$, see figure 17.

Observe that $\dim(\mathcal{T}_1^1) = 2$, therefore there must be a relation between z_0 , z_1 and z_2 . This relation is

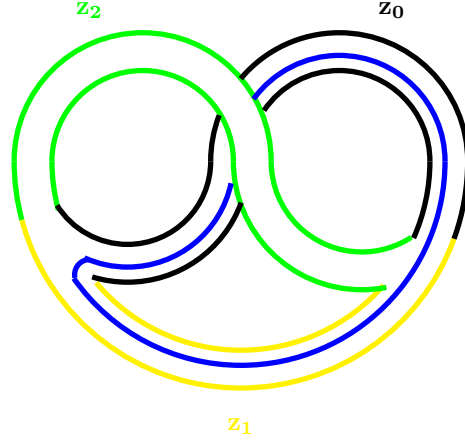
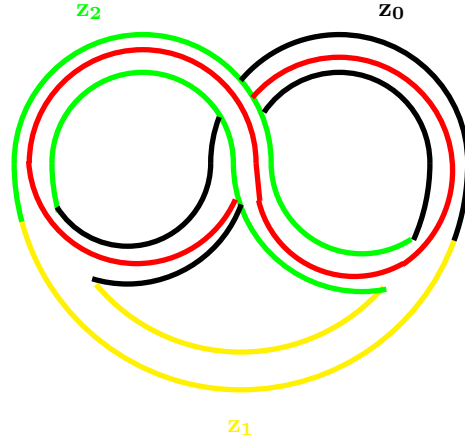
$$z_0 + z_1 + z_2 = l_P$$

where l_P is the length of the bottleneck curve P . In fact

$$\text{Tr}(LX_{z_2}LX_{z_1}LX_{z_0}LX_{z_2}LX_{z_1}LX_{z_0}) = 2\cosh(z_0 + z_1 + z_2),$$

and drawing it in the fat-graph we see that this loop unwinds itself so that it is homotopic to the hole.

In the general case one can prove the following:

FIGURE 16. Prezzle with the geodesic corresponding to γ_B .FIGURE 17. Prezzle with the geodesic corresponding to γ_A .

Theorem 2.2. Let $F_g^s = \mathbb{H}/\Delta_{g,s}$ and consider ANY associated fat-graph Γ_g^s . One can construct all elements of $\Delta_{g,s}$ by fixing a special starting edge in the fat-graph and considering all closed paths starting and finishing on the fixed edge. Then $\gamma \in \Delta_{g,s} = P_{z_1 z_2 \dots z_n}$ where P_{z_1, \dots, z_n} is a 2×2 matrix of the form

$$P_{z_1 z_2 \dots z_n} = R^{k_n} X_{z_n} R^{k_n-1} \dots X_{z_2} R^{k_1} X_{z_1}$$

where $k_1, k_2, \dots, k_n = 1, 2$. Moreover

$$2\cosh(l_\gamma) = \text{Tr}(P_{z_1 \dots z_n}),$$

and z_1, \dots, z_n are coordinates in the Teichmüller space extended by \mathbb{R}^s

$$\mathcal{T}_g^s \otimes \mathbb{R}^s.$$

These coordinates satisfy relations of the form

$$\text{Tr}(P_j) = \sum_{i \in I_j} z_i, \quad j = 1, \dots, s,$$

where I_j is the subset of indices labelling all edges in the face containing the j -th hole.

Remark 2.3. The number of edges in a fat-graph is $6g - 6 + 3s$ which is the dimension of $\mathcal{T}_g^s \otimes \mathbb{R}^s$. For the i -th edge we have a label z_i , so that we have $6g - 6 + 3s$ edges satisfying s relations. These are enough to determine $\Delta_{g,s}$ uniquely. In fact, if we know for example that the closed path corresponding to γ passes through the edges x and y , we also know k_x and k_y because each vertex is trivalent, so to go from x to y there only one possible turn.

Example 2.4. We present here the fat graph corresponding to a Riemann surface of genus 2 with two holes. The geodesic drawn in the picture is uniquely determined by the vertical edges i, j it passes through. To count the number of faces one is to start on one of the boundaries and follow it. The number of faces is given by the number of distinct closed loops we can construct in this way.

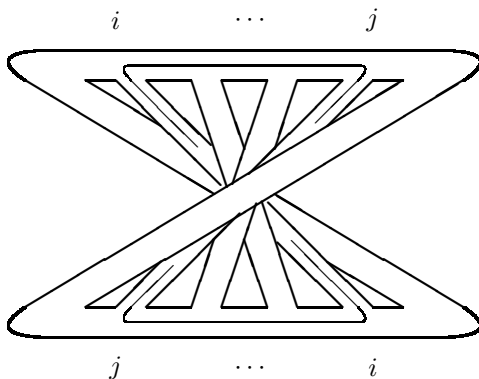


FIGURE 18. Fat graph corresponding to a Riemann surface of genus 2 with two holes.

3. MODULAR GROUP ACTION

Let us draw the attention now to the word “ANY” in the statement of Theorem 2.2. This corresponds to the fact that our splitting of the crossings in the fat-graph was arbitrary. Choosing a different splitting corresponds to perform a transformation that preserves all geodesics and all traces, i.e. to the action of the modular group $\mathbb{P}SL(2, \mathbb{R})$.

On the fat-graph changing the splitting of the crossing means that the edge which was on top, now goes on the bottom and viceversa, as in figure 19

We can visualize this edge flip by representing the prezzle itself as a graph. In fact as we saw in figure 10, the fat graph is equivalent to a choice of the way of resolving the crossing of the bouquet of cycles associated to our Riemann surface. Schematically we can visualize such resolving of the crossing as in figure 20.

A different resolving of the crossing leads to another prezzle as in figure 19 and to another graph as in figure 21.

Observe that the torus example is special in the sense that each couple of edges intersect twice. In general we'll have 5 different labels z_0, z_1, z_2, z_3, z_4 . The labels are by convention fixed like in figure 22.

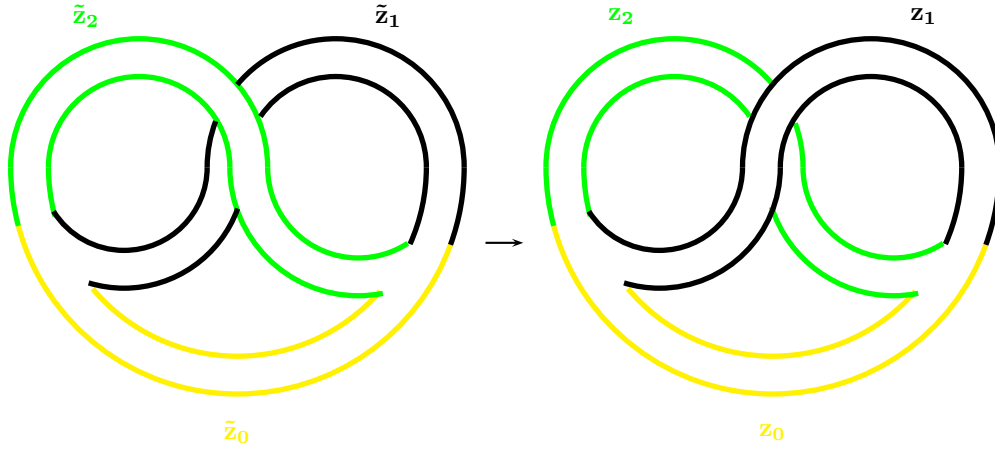


FIGURE 19. Flip

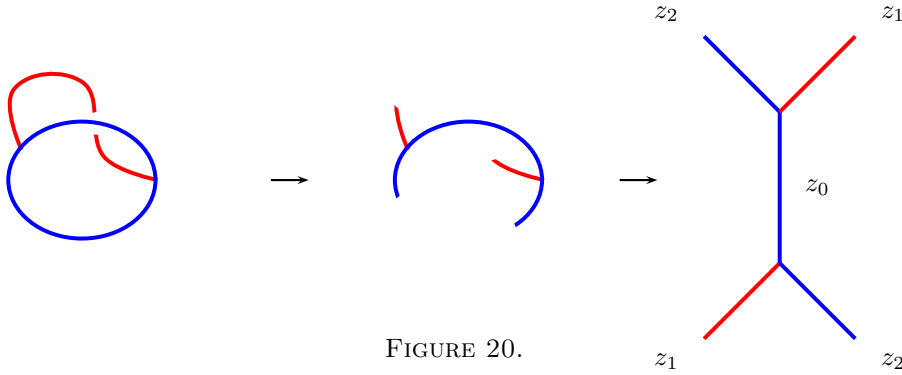


FIGURE 20.

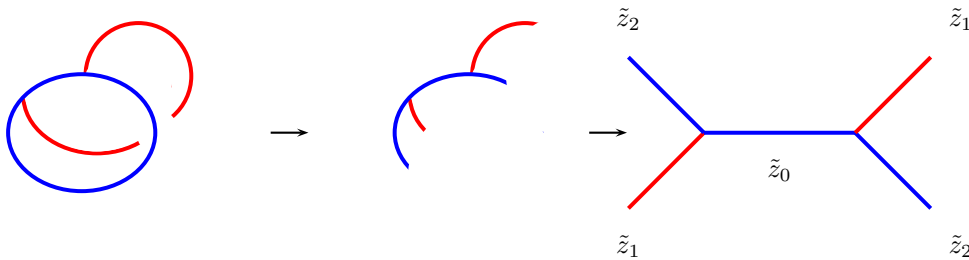


FIGURE 21.

To find the way in which the labels are transformed, it is useful to realize that a different splitting of the crossing corresponds to a different ideal triangulation of the hyperbolic plane in triangles as described in figure 22.

If we denote the vertices $-1, 0, e^{z_0}, \infty$ by x_1, \dots, x_4 , we see that the first splitting gives the *four-term relation*¹

$$\frac{(x_2 - x_1)(x_4 - x_3)}{(x_3 - x_2)(x_4 - x_1)} = e^{-z_0},$$

¹In the standard terminology, variables z_i are called the shear coordinates.

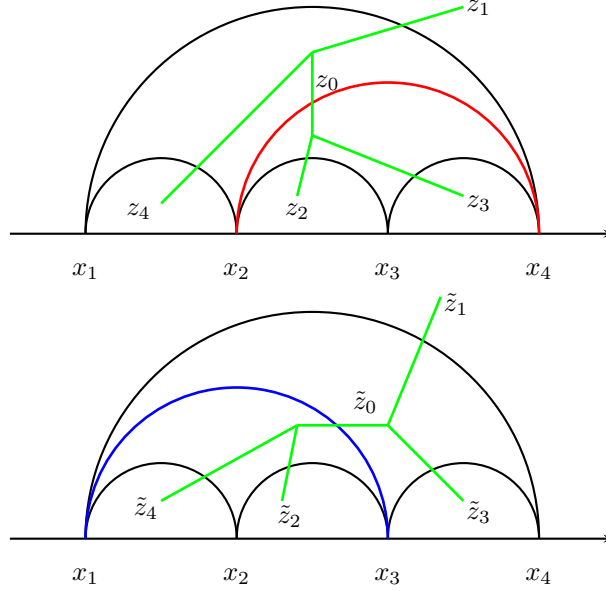


FIGURE 22.

while the second gives

$$\frac{(x_3 - x_2)(x_4 - x_1)}{(x_4 - x_3)(x_2 - x_1)} = e^{z_0},$$

so that the flip corresponds to map $z_0 \rightarrow -z_0$. Let us see how z_2 changes. To this aim, let us pick a fifth point x_5 , such that $x_2 < x_5 < x_3$ and construct the hyperbolic triangle with vertices x_2, x_5, x_3 . If we look under the microscope, we see that the initial configuration for z_2 is the same as the z_0 configuration in the bottom of figure 22 in which the point labels are changed as

$$x_1 \rightarrow x_2, \quad x_2 \rightarrow x_5, \quad x_3 \rightarrow x_3, \quad x_4 \rightarrow x_4.$$

So by the four-term relation we get

$$\frac{(x_4 - x_3)(x_5 - x_2)}{(x_3 - x_5)(x_4 - x_2)} = e^{z_2}.$$

In the same way, the final configuration for \tilde{z}_2 is the same as the z_0 configuration in the top figure 22, again with points changed as

$$x_1 \rightarrow x_1, \quad x_2 \rightarrow x_2, \quad x_3 \rightarrow x_5, \quad x_4 \rightarrow x_3.$$

So:

$$\frac{(x_5 - x_2)(x_3 - x_1)}{(x_2 - x_1)(x_3 - x_5)} = e^{-\tilde{z}_2}.$$

It is a straightforward computation to show that then $\tilde{z}_2 = z_2 + \varphi(z_0)$ where $\varphi(z_0) = \log(1 + e^{z_0})$. One can prove analogous relations for \tilde{z}_1, \tilde{z}_3 and \tilde{z}_4 . These are represented in figure 23.

In the torus situation, every edges meets every other one twice. This means that we have to sum the contributions. In fact, for example $z_2 = z_4$. Therefore we have a double contribution $2\varphi(z)$. This is shown in figure 24.

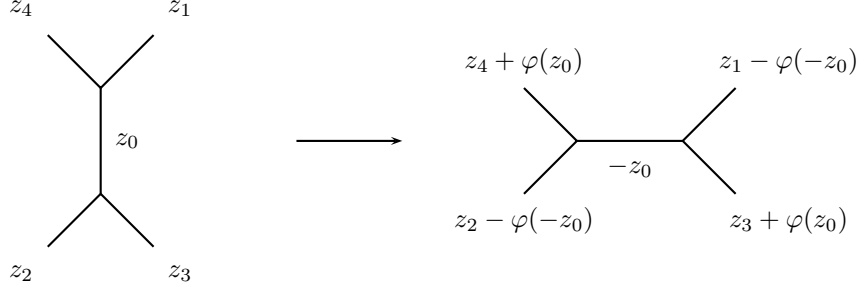


FIGURE 23. The flip in the general situation.

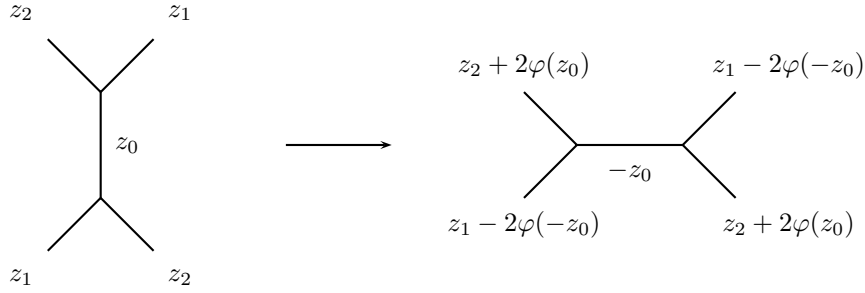


FIGURE 24. The flip in the torus situation.

Let us see how to produce a mapping class group transformation from a flip morphism. We call it “morphism” because it establishes a relation between two specific graphs. Denote the morphism between two graphs Γ_1 and Γ_2 by $[\Gamma_1, \Gamma_2]$. Suppose we have a sequence of morphisms between graphs of the same combinatorial type (i.e. only the labels are different):

$$[\Gamma_1, \Gamma_2], [\Gamma_2, \Gamma_3], \dots, [\Gamma_{n-1}, \Gamma_n],$$

denote by $z_\alpha^{(k)}$ the labels of the k -th graph Γ_k . We want to show that $z_\alpha^{(n)}$ is obtained from $z_\beta^{(1)}$ by the action of the mapping class group. Again we do it in our example \mathcal{T}_1^1 .

Under this map the order of z_0, z_1, z_2 must be preserved: since before the mapping class group transformation, by a anti-clockwise rotation, we have the order z_0, z_1, z_2 , and after the mapping class group transformation, we have the order $-z_0, z_2 + 2\varphi(z), z_1 - 2\varphi(-z)$, we see that the map is

$$z_0 \mapsto -z_0, \quad z_1 \mapsto z_2 + 2\log(1 + e^{z_0}), \quad z_2 \mapsto z_1 - 2\log(1 + e^{-z_0}),$$

so that $z_0 + z_1 + z_2$ remains invariant and the orientation is preserved.

Let $U = \exp(\frac{z_0}{2})$, $V = \exp(\frac{z_2}{2})$, then

$$U \mapsto U^{-1},$$

and

$$V \mapsto \frac{e^{\frac{z_1}{2}}}{1 + e^{-z_0}} = e^{\frac{l_P}{2}} \frac{e^{-\frac{z_2}{2}} e^{-\frac{-z_0}{2}}}{1 + e^{-z_0}} = e^{\frac{l_P}{2}} \frac{V^{-1}}{U + U^{-1}},$$

so that indeed we have a modular transformation. This is in fact a general statement.

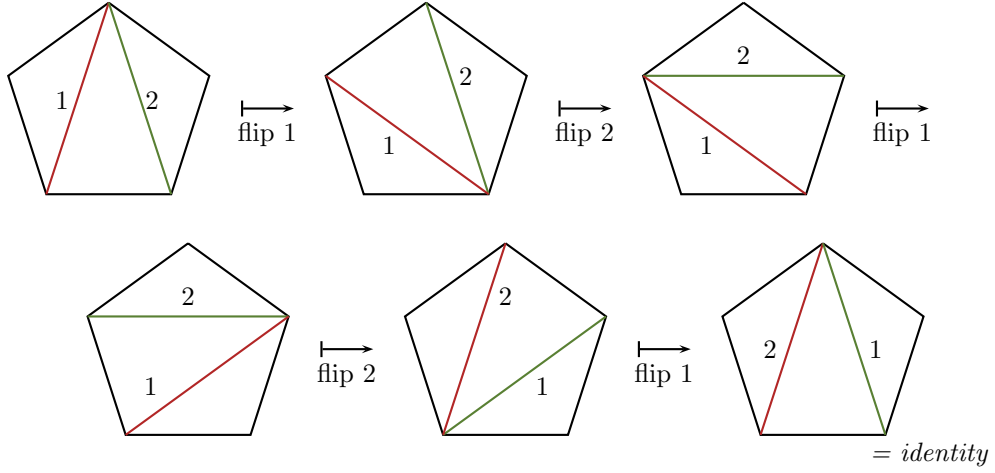
The next theorem is valid in the general situation of SINGLE intersection (not for the torus!):

Theorem 3.1. [12, 13] *The following special relations between morphisms hold true:*

- (1) *The flips are in involution:*

$$[\Gamma_1, \Gamma_2][\Gamma_2, \Gamma_1] = \text{Id},$$

- (2) *Four-term relation: flips of disjoint edges commute.*
 (3) *Pentagon identity (valid for flips of two edges having a single common vertex):*



4. POISSON BRACKETS

Since quantization is our ultimate aim, we need to select an appropriate set of observables. The natural observables of the theory are the lengths of the closed geodesics. We shall denote a collection of labels by $P = \{z_{i_1}, \dots, z_{i_n}\}$, and identify it with the corresponding matrix $P = R^{k_n} X_{z_{i_n}} R^{k_{n-1}} \dots X_{z_{i_2}} R^{k_1} X_{z_{i_1}}$. We'll denote by G_P the length of the geodesic γ_P passing through the edges $\{z_{i_1}, \dots, z_{i_n}\}$.

We postulate the Poisson brackets between edges as follows: we establish an ordering, for example anticlockwise, at each edge, so that we label the edges concurring at the same vertex by z_1, z_2, z_3 . Then we establish

$$(1) \quad \{z_i, z_{i+1}\} = 1.$$

To find the Poisson bracket between two edges, we need to sum on all common vertices. In our example of the torus with one hole we get

$$\{z_0, z_1\} = \{z_1, z_2\} = \{z_2, z_0\} = 2.$$

Theorem 4.1. *The only central elements of the given Poisson algebra are $\text{Tr}(P_j) = \sum_{i \in I_j} z_i$, $j = 1, \dots, s$, where I_j is the subset of indices labeling all edges in the face containing the j -th hole.*

Corollary 4.2. *The dimension of the symplectic leaves is equal to the dimension of the Teichmüller space, which is $6g - 6 + 2s$.*

4.1. **Relations between geodesic functions.** Let us first deal with the case of one intersection.

- Skein–relation:

$$G_P G_Q = G_{PQ} + G_{PQ^{-1}}.$$

This corresponds to the relation

$$\mathrm{Tr}(PQ) + \mathrm{Tr}(PQ^{-1}) = \mathrm{Tr}(P)\mathrm{Tr}(Q),$$

valid for matrices having determinant equal to one. Graphically it means that we split the crossing in two possible ways (see figure 25).

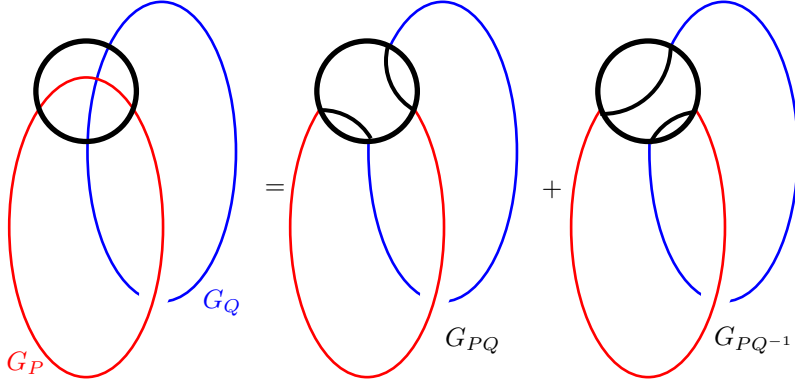


FIGURE 25. Skein relation.

- Poisson bracket: it is induced by bracket (1)²

$$(2) \quad \{G_P, G_Q\} = \frac{1}{2}G_{PQ} - \frac{1}{2}G_{PQ^{-1}}.$$

This is precisely the Goldman bracket on the space of geodesic functions in 2 + 1–gravity. It comes from the assumption (1). This is visualized graphically as in figure 26. To remember this rule we fix an orientation on γ_P and establish to assign a + when we turn left and a minus when we turn right. Observe that since $\mathrm{Tr}(P) = \mathrm{Tr}(P^{-1})$, this Poisson bracket does not depend on the orientation of the loops γ_P and γ_Q .

Example 4.3. Let us show that the Poisson bracket between geodesics coincides with (1) in the special case of $P = \gamma_A = LX_{z_2}RX_{z_0}$ and $Q = \gamma_B = RX_{z_1}LX_{z_0}$

$$P = \begin{pmatrix} e^{-\frac{z_2}{2} - \frac{z_0}{2}} & -e^{-\frac{z_2}{2} + \frac{z_0}{2}} \\ -e^{-\frac{z_2}{2} - \frac{z_0}{2}} & e^{-\frac{z_2}{2}}(e^{\frac{z_2}{2}} + e^{-\frac{z_2}{2}}) \end{pmatrix}, \quad Q = \begin{pmatrix} e^{-\frac{z_0}{2}}(e^{-\frac{z_1}{2}} + e^{\frac{z_1}{2}}) & -e^{\frac{z_1}{2} + \frac{z_0}{2}} \\ -e^{\frac{z_1}{2} - \frac{z_0}{2}} & e^{\frac{z_1}{2} + \frac{z_0}{2}} \end{pmatrix},$$

$$\begin{aligned} \{\mathrm{Tr}(P), \mathrm{Tr}(Q)\} &= \frac{\partial \mathrm{Tr}(P)}{\partial z_2} \frac{\partial \mathrm{Tr}(Q)}{\partial z_0} \{z_2, z_0\} + \frac{\partial \mathrm{Tr}(P)}{\partial z_0} \frac{\partial \mathrm{Tr}(Q)}{\partial z_1} \{z_0, z_1\} + \\ &\quad + \frac{\partial \mathrm{Tr}(P)}{\partial z_2} \frac{\partial \mathrm{Tr}(Q)}{\partial z_1} \{z_2, z_1\} = \\ &= \frac{1}{2}e^{-\frac{z_2}{2} - \frac{z_1}{2} - z_0} (1 + e^{z_1} - e^{z_0} - e^{z_0+z_2} + 2e^{z_1+z_0} - e^{z_2+z_1+z_0} + e^{z_1+2z_0} + e^{z_2+z_1+2z_0}). \end{aligned}$$

²See the calculation in Appendix B.

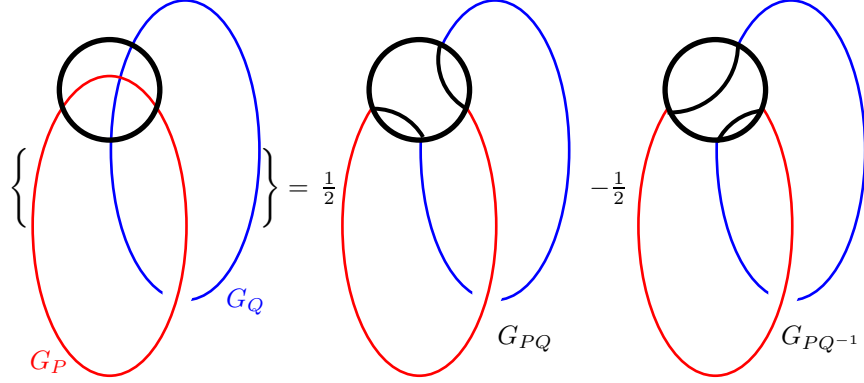


FIGURE 26. Poisson bracket.

Now, using (2), and observing that

$$PQ = \begin{pmatrix} e^{-\frac{z_2}{2} + \frac{z_1}{2}} + e^{-\frac{z_2}{2} - \frac{z_1}{2} - z_0} + e^{-\frac{z_2}{2} + \frac{z_1}{2} - z_0} & -e^{-\frac{z_2}{2} + \frac{z_1}{2}} - e^{-\frac{z_2}{2} + \frac{z_1}{2} + z_0} \\ -e^{-\frac{z_2}{2} + \frac{z_1}{2}} - e^{\frac{z_2}{2} + \frac{z_1}{2}} - e^{-\frac{z_2}{2} - \frac{z_1}{2} - z} - e^{-\frac{z_2}{2} + \frac{z_1}{2} - z_0} & e^{-\frac{z_2}{2} + \frac{z_1}{2}} + e^{-\frac{z_2}{2} + \frac{z_1}{2} + z_0} + e^{\frac{z_2}{2} + \frac{z_1}{2} + z_0} \end{pmatrix},$$

$$PQ^{-1} = \begin{pmatrix} 0 & -e^{-\frac{z_2}{2} - \frac{z_1}{2}} \\ e^{\frac{z_2}{2} + \frac{z_1}{2}} & e^{-\frac{z_2}{2} - \frac{z_1}{2}} + e^{\frac{z_2}{2} - \frac{z_1}{2}} + e^{\frac{z_2}{2} + \frac{z_1}{2}} \end{pmatrix},$$

we obtain the same result.

Let us show that this Poisson bracket is skew symmetric: in fact graphically $\{G_Q, G_P\}$ means that γ_Q is now on top: fix any direction on γ_Q and assign a + when we turn left and a minus when we turn right as above.

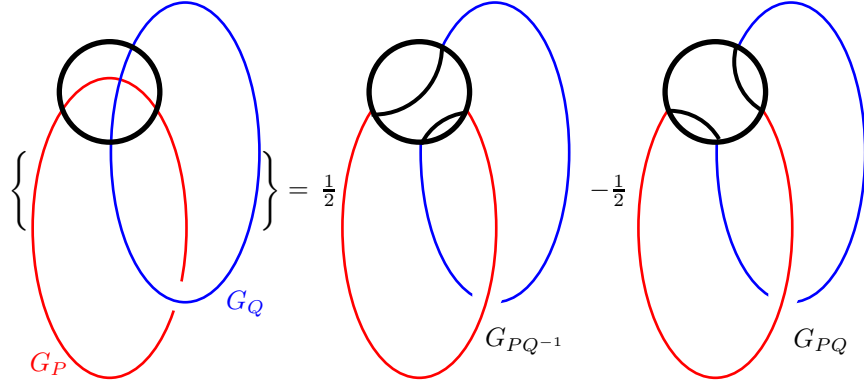


FIGURE 27. Poisson bracket.

The main problem is to close this Poisson algebra by using the skein relation. That is, we want to choose a “basis” of geodesic functions, such that their Poisson brackets are expressed in terms of the basis elements only. We quote the word “basis” because the number of elements in it is actually larger than the dimension.

Example 4.4. In our torus with one hole we choose the "basis" given by $G_{z_2 z_1}$, $G_{z_1 z_0}$, $G_{z_0 z_2}$. We get

$$\{G_{z_2 z_1}, G_{z_1 z_0}\} = \frac{1}{2}G_{z_0 z_2} - \frac{1}{2}G_{z_2 z_1 z_0 z_1},$$

and by using the skein relation

$$\{G_{z_2 z_1}, G_{z_1 z_0}\} = \frac{1}{2}G_{z_2 z_1} G_{z_1 z_0} - \frac{1}{2}G_{z_0 z_2},$$

The central element of this algebra is

$$G_{z_2 z_1}^2 + G_{z_1 z_0}^2 + G_{z_0 z_2}^2 - G_{z_2 z_1} G_{z_1 z_0} G_{z_0 z_2}.$$

Definition 4.5. A geodesic is called *graph simple* if it does not pass twice through the same edge.

Example 4.6. In our torus with one hole we have only 3 graph-simple geodesics, the A -cycle A , the B -cycle B and AB^{-1} . Their lengths generate the algebra

$$\begin{aligned} \{G_A, G_B\} &= \frac{1}{2}G_A G_B - G_{AB^{-1}}, \\ \{G_B, G_{AB^{-1}}\} &= \frac{1}{2}G_B G_{AB^{-1}} - G_A, \\ \{G_{AB^{-1}}, G_A\} &= \frac{1}{2}G_A G_{AB^{-1}} - G_B. \end{aligned}$$

In the case of higher genus and $s = 1, 2$, Chekhov and Fock have proved that the algebra is always closed by choosing the set of graph-simple geodesics.

Definition 4.7. A *geodesic lamination* GL is a set of non-(self)-intersecting geodesics. The associated algebraic object \mathcal{GL} is the product of their lengths.

$$\mathcal{GL} := \prod_{\gamma \in GL} G_\gamma.$$

The advantage of considering geodesic laminations is that all relations are linear:

$$\mathcal{GL}_1 \mathcal{GL}_2 = \sum_j c_{12}^j \mathcal{GL}_j, \quad \{\mathcal{GL}_1, \mathcal{GL}_2\} = \sum_j \tilde{c}_{12}^j \mathcal{GL}_j,$$

where the constants $c_{il}^j \in \mathbb{Z}$ and $\tilde{c}_{il}^j \in \frac{1}{2}\mathbb{Z}$.

The disadvantage is that the geodesic laminations can be chosen in infinite ways, therefore they are not algebraically independent.

5. QUANTIZATION

We quantize using the correspondence principle: to each coordinate z_α we associate a Hermitean operator Z_α^{\hbar} such that the set of these Hermitean operators forms a C^* -algebra (in our case the algebra of operators on $L^2(3g - 3 + s)$). We postulate the commutation relations between Hermitean operators as follows:

$$(2) \quad [Z_\alpha^{\hbar}, Z_\beta^{\hbar}] = 2\pi i \hbar \{z_\alpha, z_\beta\}.$$

The central elements of this algebra are the quantum analogues of the Casimirs. They are mapped to

$$P_j^{\hbar} = \sum_{i \in I_j} Z_i^{\hbar}, \quad j = 1, \dots, s,$$

where I_j is the subset of indices labeling all edges in the face containing the j -th hole. Observe that in the quantum picture we lose the geometric picture: we're left only with an abstract algebra.

The quantum morphisms work in the same way as before, with the quantum analogue of ϕ which we denote by Φ^{\hbar} . This function must satisfy the following properties:

- (1) $\Phi^{\hbar}(z) - \Phi^{\hbar}(-z) = z$ to preserve the commutation relations.
- (2) Semiclassical limit: $\lim_{\hbar \rightarrow 0} \Phi^{\hbar}(z) = \varphi(z)$.
- (3) Quantum pentagon identity. This is non-trivial as the quantized variables Z_{α}^{\hbar} don't commute.

Let us see how to prove the first property. We assume the quantum flip to work similarly to the classical one, as described in figure 28.

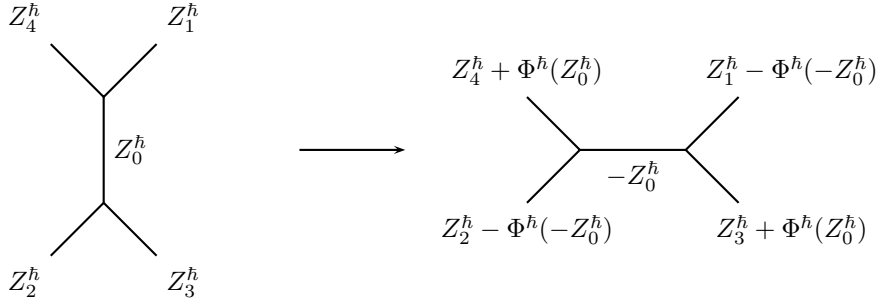


FIGURE 28. The quantum flip in the general situation.

Say we wish to preserve the commutation relation

$$[Z_1^{\hbar}, Z_4^{\hbar}] = 2\pi i.$$

As we have seen just before Theorem 3.1, $Z_1^{\hbar} \rightarrow Z_4^{\hbar} + \Phi^{\hbar}(Z_0^{\hbar})$ and $Z_4^{\hbar} \rightarrow Z_2^{\hbar} - \Phi^{\hbar}(-Z_0^{\hbar})$, so that we want

$$[Z_4^{\hbar} + \Phi^{\hbar}(Z_0^{\hbar}), Z_2^{\hbar} - \Phi^{\hbar}(-Z_0^{\hbar})] = 2\pi i.$$

Since $[Z_4^{\hbar}, Z_2^{\hbar}] = 0$, this means that we want:

$$[Z_4^{\hbar}, -\Phi^{\hbar}(-Z_0^{\hbar})] + [\Phi^{\hbar}(Z_0^{\hbar}), Z_2^{\hbar}] = 2\pi i,$$

and by the postulated commutation relations (3), we get

$$\frac{d}{dZ_0^{\hbar}} (-\Phi^{\hbar}(-Z_0^{\hbar}) + \Phi^{\hbar}(Z_0^{\hbar})) = 1,$$

which proves the first property after integration in Z_0^{\hbar} .

One can prove that a good candidate for Φ^{\hbar} is the *quantum dilogarithm function* [9] (a.k.a. the Barnes function in mathematical literature):

$$\Phi^{\hbar}(z) := -\frac{\pi\hbar}{2} \int \frac{e^{-ipz} dp}{\sinh(\pi p) \sinh(\pi p \hbar)}.$$

This function has two properties of quasi-periodicity:

$$\Phi^{\hbar}(z + i\pi\hbar) - \Phi^{\hbar}(z - i\pi\hbar) = \frac{2\pi i \hbar}{1 + e^{-z}}, \quad \Phi^{\hbar}(z + i\pi) - \Phi^{\hbar}(z - i\pi) = \frac{2\pi i}{1 + e^{-\frac{z}{\hbar}}}.$$

The quantum geodesic functions will be operators. Recall that at classical level the geodesic functions were $G\gamma = 2 \cosh(\frac{l_{\gamma}}{2}) = \text{Tr}(P_{z_1, \dots, z_n})$. When we quantize

the quantized Z_α^{\hbar} do not commute anymore: we have to choose an ordering in the trace. We'll denote the quantum ordering by

$$\underset{\text{X}}{\overset{\text{X}}{\text{Tr}}}(P_{Z_1 \dots Z_n})$$

In the classical case we had that $G\gamma$ was a sum of exponential terms of integer or half integer linear combinations of z_1, \dots, z_n . Now in the quantum case we can no longer use the property that $e^a e^b = e^{a+b}$, so we'll need to add a term $2\pi i \hbar C(\gamma, \alpha)$, which will depend on the geodesic γ and on the set of edges α it passes through.

This is difficult to compute. However thanks to the fact that the quantized operators Z_α^{\hbar} are Hermitean, one can prove a few results. In particular, if we restrict to the class of *graph-simple geodesics*, i.e. geodesics which pass through one edge only once, then $C(\gamma, \alpha) = 0$ so that the quantum ordering is Weyl ordering and we have the Moyal product.

Skein relation and Poisson bracket are now encoded in a single *quantum skein relation*, which for one crossing is given in figure 29 in which $q = e^{-i\pi\hbar}$, so that for $q = 1$ we get the classical skein relation and the first correction in \hbar produces the Poisson bracket.

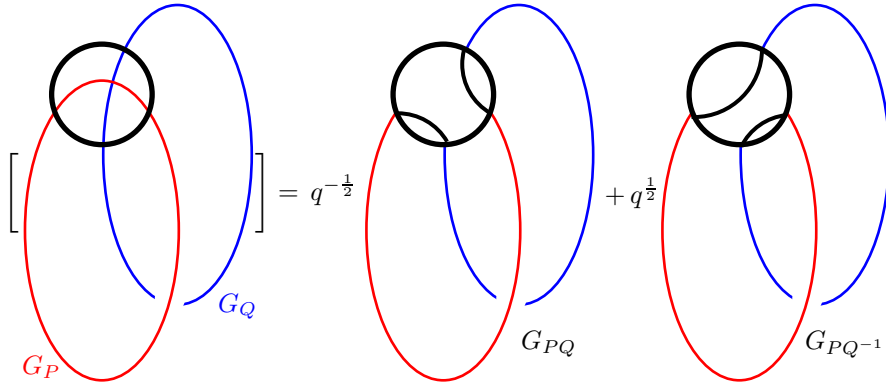


FIGURE 29. Quantum version of skein relation and Poisson bracket.

We need to assign a geodesic length to the empty loop too. This is fixed to be equal to -2 in the classical case, and it becomes $-q - q^{-1}$ in the quantum case. The reason for this is described in figure 30, in which we consider two a priori commuting geodesic functions and compute their quantum skein relation.

Let us see how to close the algebra in the quantum case. In fact before we had two relations, i.e., the Poisson bracket and the skein relation. When computing the former, we used the latter to replace unwanted terms. But now we have only one relation, so what shall we do? The trick is to use the non-commutativity, i.e. to use the quantum skein relation twice, once for $G_A G_B$ and once for $G_B G_A$:

$$G_A G_B = q^{-\frac{1}{2}} G_{AB} + q^{\frac{1}{2}} G_{AB^{-1}}, \quad G_B G_A = q^{\frac{1}{2}} G_{AB} + q^{-\frac{1}{2}} G_{AB^{-1}},$$

so that if we define the quantum commutator as

$$[G_A, G_B]_q := q^{\frac{1}{2}} G_A G_B - q^{-\frac{1}{2}} G_B G_A,$$

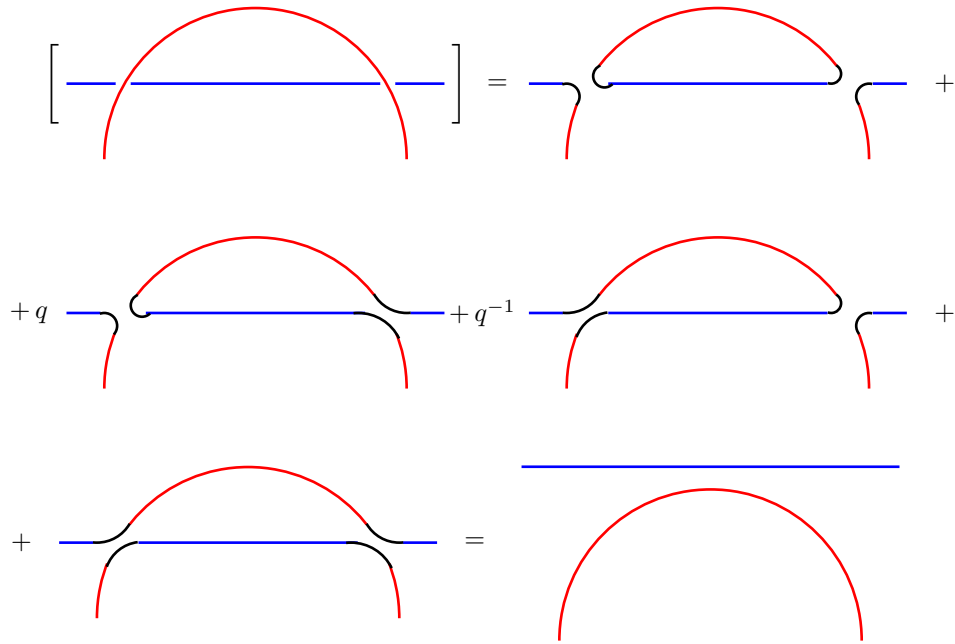


FIGURE 30. Quantum Whitehead move I: it holds if the empty loop is $-q - q^{-1}$.

we get

$$[G_A, G_B]_q := (q^{\frac{1}{2}} - q^{-\frac{1}{2}})G_{AB^{-1}}.$$

6. BIBLIOGRAPHIC REFERENCES

The combinatorial description of Teichmüller theory was proposed by R.C. Penner [11, 12, 13] in the case of punctured surfaces and was advanced by V.V. Fock [1, 2] for the case of surfaces with holes.

The Poisson algebras of geodesic functions have a long history, first, irrespectively on the combinatorial description. Their investigation has been started in the $2 + 1$ gravity pattern in which W. Goldman [14] established his famous Goldman bracket. Using it, J. Nelson and T. Regge (subsequently in collaboration with S. Carlip and Zertuche) found [15, 16] algebras for a special basis of geodesic functions. The geodesic algebras were found in the graph (combinatorial) description in [4], whereas the representation in terms of the graph-simple geodesics for a general Nelson–Regge algebra was found in [5].

The quantization of the Teichmüller space coordinates satisfying the pentagon identity was proposed by Chekhov and Fock [3] and independently by Kashaev [6]. The quantum dilogarithm function in the modern concept was introduced by L.D. Faddeev [9] in his studies of the quantum Heisenberg algebra symmetries. A good accounting for representations of quantum geodesic functions and of their spectral properties is in [7].

Further development of this activity was the quantization of the Thurston theory [8], the Fock–Goncharov construction for quantizing $PSL(n, \mathbb{R})$ and other algebras [17], generalizations to the bordered surfaces case, etc. The Nelson–Regge algebras

has appeared as algebras of the upper-triangular groupoid [18] and of the Stokes parameters [19] for the Frobenius manifolds.

APPENDIX A. THE HYPERBOLIC METRIC

The *hyperbolic distance* $\rho(z, w)$ between two points $z, w \in \mathbb{H}$ is defined as the length of the geodesic connecting them. This defines \mathbb{H} as a metric space. It is a straightforward computation to show that

$$\rho(z, w) = \ln \left(\frac{|z - \bar{w}| + |z - w|}{|z - \bar{w}| - |z - w|} \right),$$

so that

$$\sinh^2 \left(\frac{1}{2} \rho(z, w) \right) = \frac{|z - w|^2}{4 \operatorname{Im}(z) \operatorname{Im}(w)}.$$

Using this formula we are now going to show that the topology induced by the hyperbolic distance on \mathbb{H} is the same as the one induced by the Euclidean metric. In fact a hyperbolic circle is also a Euclidean circle and vice versa. Let us see this in an example: consider the hyperbolic circle C of center i and radius δ :

$$C = \left\{ z \in \mathbb{H} \mid \sinh^2 \left(\frac{1}{2} \rho(z, i) \right) = \sinh^2 \left(\frac{\delta}{2} \right) \right\}.$$

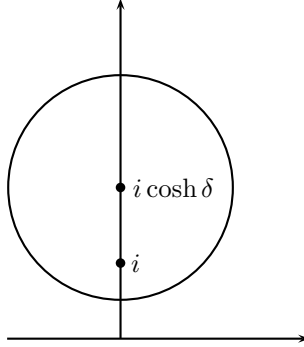


FIGURE 31.

Clearly we get

$$\begin{aligned} C &= \left\{ z = x + iy \mid |z - i|^2 = 4y \sinh^2 \left(\frac{\delta}{2} \right) \right\} = \\ &= \left\{ z = x + iy \mid x^2 + y^2 + 1 = 2y \left(2 \sinh^2 \left(\frac{\delta}{2} \right) + 1 \right) = 2y \cosh \delta \right\} = \\ &= \left\{ z = x + iy \mid x^2 + (y - \cosh \delta)^2 = \cosh^2 \delta - 1 = \sinh^2 \delta \right\}. \end{aligned}$$

Therefore C is a Euclidean circle of center $z = i \cosh \delta$ and radius $\sinh \delta$.

APPENDIX B. POISSON BRACKETS BETWEEN GEODESIC FUNCTIONS

We now calculate the Poisson bracket between geodesic functions labeled “1” and “2” and having a crossing as indicated in figure 32.

We use the following notation standard, for example, in integrable systems. We treat matrix elements of the first and second geodesic functions as linear operators in two different two-dimensional spaces. The superscripts “(1)” and “(2)” indicate quantities belonging to the space with the corresponding number in the direct product of spaces, $e_{ij}^{(s)}$ is the matrix in the s th space ($s = 1, 2$) with the only nonzero entry to be the unity on the crossing of i th row and j th column, and ε_{ij} is the totally antisymmetric tensor (with $\varepsilon_{12} = 1$). Every operator acting in the direct product of spaces can be decomposed over the basis with the basic vectors to be $e_{ij}^{(1)} \otimes e_{kl}^{(2)}$, $i, j, k, l = 1, 2$. We also distinguish between evaluating traces in these two spaces.

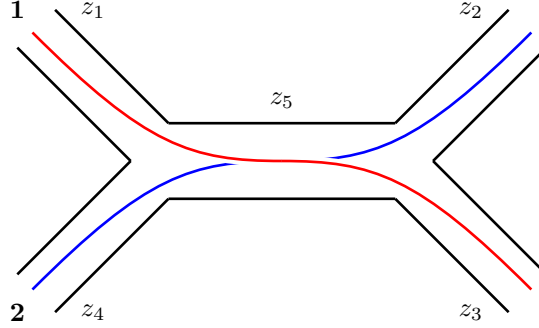


FIGURE 32.

Another way to represent X_z is

$$X_z^{(1)} = \sum_{i,j=1}^2 (-1)^{\varepsilon_{ij}+1} e^{\varepsilon_{ij}z/2} e_{ij}^{(1)}.$$

Then,

$$\{X_{z_1}^{(1)}, X_{z_4}^{(2)}\} = \frac{-1}{4} X_{z_1}^{(1)} \otimes X_{z_4}^{(2)} \mathcal{S}^{12},$$

where z_1 and z_4 are as in figure 32 and

$$\mathcal{S}^{12} := e_{11}^{(1)} \otimes e_{11}^{(2)} - e_{22}^{(1)} \otimes e_{11}^{(2)} - e_{11}^{(1)} \otimes e_{22}^{(2)} + e_{22}^{(1)} \otimes e_{22}^{(2)}$$

is a diagonal matrix. Note that

$$(A.4) \quad X_{z_1}^{(1)} \otimes X_{z_4}^{(2)} \mathcal{S}^{12} = \mathcal{S}^{12} X_{z_1}^{(1)} \otimes X_{z_4}^{(2)},$$

so we can put the matrix \mathcal{S}^{12} from any side of this tensorial product. When calculating the Poisson brackets between geodesic functions $G_1 = \text{Tr}P$ and $G_2 = \text{Tr}Q$ in figure 32, we insert a proper number (six in this case) of the matrices \mathcal{S}^{12} in the tensorial product of

$$P^{(1)} \otimes Q^{(2)} = \dots X_{z_3}^{(1)} R^{(1)} X_{z_5}^{(1)} L^{(1)} X_{z_1}^{(1)} \dots \otimes \dots X_{z_2}^{(2)} L^{(2)} X_{z_5}^{(2)} R^{(2)} X_{z_4}^{(2)} \dots;$$

due to the property (A.4) all these insertions can be done to the right from $X_{z_3}^{(1)}$ and $X_{z_2}^{(2)}$ and to the left from $X_{z_1}^{(1)}$ and $X_{z_4}^{(2)}$. We show these insertions schematically on the figure 33, where the signs (+) and (-) indicate with which sign the corresponding matrix \mathcal{S}^{12} enters the direct product. Eventually, using that $X_z X_z = RL = LR = -\mathbf{1}$, we push all \mathcal{S}^{12} insertions to the single place just to the right from $X_{z_5}^{(1)} \otimes X_{z_5}^{(2)}$. We then have for the bracket

$$\begin{aligned} & \dots \frac{1}{4} (RX_{z_5})^{(1)} \otimes (LX_{z_5})^{(2)} \left\{ (X_{z_5}L)^{(1)} \otimes \mathbf{1}^{(2)} \mathcal{S}^{12} (RX_{z_5})^{(1)} \otimes \mathbf{1}^{(2)} \right. \\ & - (X_{z_5}L)^{(1)} \otimes (X_{z_5}R)^{(2)} \mathcal{S}^{12} (RX_{z_5})^{(1)} \otimes (LX_{z_5})^{(2)} + X_{z_5}^{(1)} \otimes R^{(2)} \mathcal{S}^{12} X_{z_5}^{(1)} \otimes L^{(2)} \\ & + \mathbf{1}^{(1)} \otimes (X_{z_5}R)^{(2)} \mathcal{S}^{12} \mathbf{1}^{(1)} \otimes (LX_{z_5})^{(2)} + L^{(1)} \otimes X_{z_5}^{(2)} \mathcal{S}^{12} R^{(1)} \otimes X_{z_5}^{(2)} \\ & \left. - L^{(1)} \otimes R^{(2)} \mathcal{S}^{12} R^{(1)} \otimes L^{(2)} \right\} L^{(1)} \otimes R^{(2)} \dots \end{aligned}$$

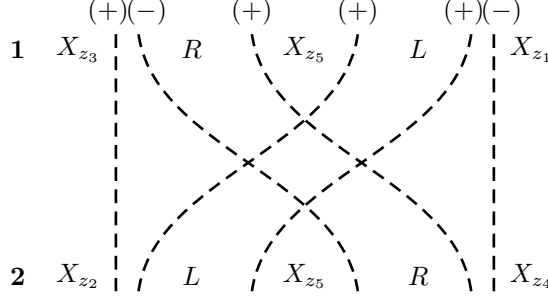


FIGURE 33.

It remains just to calculate explicitly the part in the brackets. It reads

$$\begin{aligned} & \begin{pmatrix} 1 & -2e^{z_5} \\ 0 & -1 \end{pmatrix} \otimes \begin{pmatrix} 1 & 0 \\ 2e^{-z_5} & -1 \end{pmatrix} + \begin{pmatrix} 1 & -2e^{z_5} \\ 0 & -1 \end{pmatrix} \otimes \begin{pmatrix} 1 & 0 \\ 0 & -1 \end{pmatrix} \\ & + \begin{pmatrix} 1 & 0 \\ 0 & -1 \end{pmatrix} \otimes \begin{pmatrix} 1 & 2 \\ 0 & -1 \end{pmatrix} + \begin{pmatrix} 1 & 0 \\ 0 & -1 \end{pmatrix} \otimes \begin{pmatrix} 1 & 0 \\ 2e^{-z_5} & -1 \end{pmatrix} \\ & + \begin{pmatrix} 1 & 0 \\ -2 & -1 \end{pmatrix} \otimes \begin{pmatrix} 1 & 0 \\ 0 & -1 \end{pmatrix} - \begin{pmatrix} 1 & 0 \\ -2 & -1 \end{pmatrix} \otimes \begin{pmatrix} 1 & 2 \\ 0 & -1 \end{pmatrix} \\ & = 4 \begin{pmatrix} 0 & e^{z_5} \\ 0 & 0 \end{pmatrix} \otimes \begin{pmatrix} 0 & 0 \\ e^{-z_5} & 0 \end{pmatrix} + 4 \begin{pmatrix} 0 & 0 \\ 1 & 0 \end{pmatrix} \otimes \begin{pmatrix} 0 & 1 \\ 0 & 0 \end{pmatrix} \\ & \quad + 2 \begin{pmatrix} 1 & 0 \\ 0 & -1 \end{pmatrix} \otimes \begin{pmatrix} 1 & 0 \\ 0 & -1 \end{pmatrix} \\ & = 4(e_{12}^{(1)} \otimes e_{21}^{(2)} + e_{21}^{(1)} \otimes e_{12}^{(2)} + e_{11}^{(1)} \otimes e_{11}^{(2)} + e_{22}^{(1)} \otimes e_{22}^{(2)}) - 2(\mathbf{1}^{(1)} \otimes \mathbf{1}^{(2)}) \\ & = 4\mathcal{R}^{12} - 2\mathbf{1}^{12}, \end{aligned}$$

where \mathcal{R}^{12} (the expression in the first brackets) is the famous permutation R -matrix³

Taking into account the factor $1/4$, we immediately obtain that

$$\begin{aligned} \{\mathrm{Tr}P^{(1)}, \mathrm{Tr}Q^{(2)}\} &= \mathrm{Tr}_1\mathrm{Tr}_2[P^{(1)} \otimes Q^{(2)}(\mathcal{R}^{12} - \frac{1}{2}\mathbf{1}^{12})] \\ &= \mathrm{Tr}PQ - \frac{1}{2}\mathrm{Tr}P \cdot \mathrm{Tr}Q, \end{aligned}$$

with the usual traces in the last line. Using the skein relation

$$\mathrm{Tr}P \cdot \mathrm{Tr}Q = \mathrm{Tr}PQ + \mathrm{Tr}PQ^{-1},$$

we come to the standard form of the Poisson bracket:

$$\{\mathrm{Tr}P, \mathrm{Tr}Q\} = \frac{1}{2}\mathrm{Tr}PQ - \frac{1}{2}\mathrm{Tr}PQ^{-1}.$$

REFERENCES

- [1] Fock V.V., Combinatorial description of the moduli space of projective structures, *arxiv:hep-th/9312193*, (1993) 1–30.
- [2] Fock V.V., Dual Teichmüller spaces, *arxiv:dg-ga/9702018v1*, (1997) 1–27.
- [3] Chekhov L.O. and Fock V.V., A quantum Teichmüller space, *Theor. Math. Phys.*, **120** (1999) 1245–1259.
- [4] Chekhov L.O. and Fock V.V., Quantum mapping class group, pentagon relation, and geodesics, *Proc. Steklov Math. Inst.*, **226** (1999) 149–163.
- [5] Chekhov L.O. and Fock V.V., Observables in 3d gravity and geodesic algebras, *Czech. J. Phys.*, **50** (2000) 1201–1208.
- [6] Kashaev R.M., Quantization of Teichmüller spaces and the quantum dilogarithm, *Lett. Math. Phys.*, **43** (1998) 105–115.
- [7] Kashaev R.M., “On the spectrum of Dehn twists in quantum Teichmüller theory” in: *Physics and Combinatorics* (2000, Nagoya), World Sci. Publ., River Edge, NJ, 2001, 63–81 (arxiv:math.QA/0008148).
- [8] Chekhov L.O. and Penner R.C., On Quantizing Teichmüller and Thurston theories , *arXiv:math.AG/0403247*, (2004) 1–64.
- [9] Faddeev L.D., The inverse scattering transform — Fourier analysis for nonlinear problems, *Lett. Math. Phys.*, **34** (1995) 249–254.
- [10] Jones G.A. and Singerman D., “Complex Functions. An algebraic and geometric viewpoint.”, Cambridge University Press, (1987).
- [11] Penner R.C. *Comm. Math. Phys.* 113299–339 The decorated Teichmüller space of Riemann surfaces 1988
- [12] Penner R.C., Weil–Petersson volumes, *J. Diff. Geom.*, **35** (1992) 559–608.
- [13] Penner R.C., Universal constructions in Teichmüller theory, *Adv. Math.*, **98** (1993) 143–215.
- [14] Goldman W.M., Invariant functions on Lie groups and Hamiltonian flows of surface group representations, *Invent. Math.*, **85** (1986) 263–302.
- [15] Nelson J.E., Regge T., Homotopy groups and (2+1)-dimensional quantum gravity, *Nucl. Phys. B*, **328** (1989) 190–199.
- [16] Nelson J.E., Regge T., Zertuche F., Homotopy groups and (2 + 1)-dimensional quantum de Sitter gravity, *Nucl. Phys. B*, **339** (1990) 516–532.
- [17] Fock V.V., Goncharov A.B., Moduli spaces of local systems and higher Teichmüller theory, *arxiv:math.AG/0311149*, (2003) 1–60.
- [18] Bondal A., “A symplectic groupoid of triangular bilinear forms and the braid groups” Preprint IHES/M/00/02 (2000).
- [19] Ugaglia M., On a Poisson structure on the space of Stokes matrices, *Int. Math. Res. Not.*, **1999** (1999) no. 9, 473–493.

³This matrix, permuting the spaces 1 and 2, has the form $\sum_{i,j=1}^2 e_{ij}^{(1)} \otimes e_{ji}^{(2)}$, and it is the simplest nontrivial matrix satisfying the celebrated Yang–Baxter equation $\mathcal{R}^{12}\mathcal{R}^{23}\mathcal{R}^{12} = \mathcal{R}^{23}\mathcal{R}^{12}\mathcal{R}^{23}$ in the direct product of three spaces.

Acknowledgments. We are grateful to James Montaldi for his help with the pictures. This work was supported by the Manchester Institute for Mathematical Sciences MIMMS, by the European Science Foundation Programme “Methods of Integrable Systems, Geometry, Applied Mathematics” (MISGAM), Marie Curie RTN “European Network in Geometry, Mathematical Physics and Applications” (ENIGMA), and by the EPSRC Fellowship EP/D071895/1.